1987Metic..22...61D

# MAJOR ELEMENT COMPOSITIONAL VARIATION WITHIN AND BETWEEN DIFFERENT LATE EOCENE MICROTEKTITE STREWNFIELDS

**Steven L. D'Hondt, Gerta Keller, and Robert F. Stallard**
*Dept. of Geological and Geophysical Sciences*
*Guyot Hall*
*Princeton University*
*Princeton, NJ 08540*

*Major element compositional overlap exists between microspherules of different microtektite layers or strewnfields. For this reason, microspherules of similar composition cannot, a priori, be assumed to belong to the same microtektite event and those of different compositions cannot, a priori, be assumed to result from different events. Nevertheless, despite major element compositional overlap between microspherules of different strewnfields, multivariate factor analysis shows microtektites and related microspherules of three stratigraphically different late Eocene layers to follow recognizably different compositional trends.*

*The microtektite population of the North American strewnfield (*Globorotalia cerroazulensis *Zone) follows compositionally well defined trends and is characterized by high concentrations of* $SiO_2$*,* $Al_2O_3$*, and* $TiO_2$*. The microspherule population of the slightly older crystal-bearing* Globorotalia cerroazulensis *Zone microspherule layer is more heterogeneous and characterized by microspherules which are relatively enriched in FeO and MgO and relatively impoverished in* $SiO_2$ *and* $TiO_2$*. The microspherule population of the oldest microspherule layer in the uppermost* Globigerapsis semiinvoluta *Zone is highly heterogeneous and characterized by microspherules which are relatively enriched in CaO and impoverished in* $Al_2O_3$ *and* $Na_2O$*. Individual microspherules of this oldest late Eocene horizon often exhibit major element compositions similar to those of the lower* Gl. cerroazulensis *Zone layer and occasionally exhibit major element compositions similar to North American layer microtektites. Nevertheless, late Eocene microspherule occurrences can be assigned to appropriate late Eocene microtektite horizons on the basis of major element compositional trends.*

## INTRODUCTION

Tektites are small glassy objects commonly believed to result from the fusion of terrestrial material by a large meteorite or comet impact (Barnes and Barnes, 1973; Glass, 1982; Shaw and Wasserburg, 1982). Microtektites are microscopic tektites, usually transparent to translucent yellow, brown, or green in color. They are commonly defined on the basis of chemical composition, shape and surface morphology, inclusion of lechatelierite particles, and association with known tektite occurrences.

Donnelly and Chao (1973) first discovered microtektites of late Eocene age at Caribbean Deep Sea Drilling Project (DSDP) Site 149. Glass and colleagues subsequently searched for and discovered microtektites of late Eocene age in sites ranging from the Caribbean across the Pacific to the Indian Ocean (Glass *et al.*, 1973, 1979, 1982; John and Glass, 1974). These late Eocene microtektite occurrences have been discovered to belong to three stratigraphically distinct microspherule layers (Keller *et al.*, 1983, 1984, 1987) and have also been discussed by Glass *et al.* (1985).

The oldest of the three late Eocene microtektite horizons is found near the top of planktonic foraminiferal *Globigerapsis semiinvoluta* Zone sediments of the western Pacific and Indian Oceans; possible microtektites are found in a coeval marine section in southern Spain. The second horizon contains predominantly crystal-bearing microspherules. This second horizon occurs in the lower *Globorotalia cerroazulensis* Zone or at the radiolarian *Calocyclas bandyca*/*Cryptopora ornata* subzone boundary of the *Thyrsocyrtis bromia* Zone (Sanfilippo *et al.*, 1985). This layer has been found in sediments of the Caribbean, Gulf of Mexico, and equatorial Pacific. The youngest of these three microtektite horizons is also found in the planktonic foraminiferal *Globorotalia cerroazulensis* Zone in sediments of the Caribbean, Gulf of Mexico, and western North Atlantic. The stratigraphy, faunal extinctions, and iridium concentrations associated with these microspherule layers are discussed in Keller *et al.* (1987).

Partly on the basis of major element microspherule composition, Glass and coworkers (Glass *et al.*, 1982, 1985) have concluded that the microspherules ascribed by Keller *et al.* to the *G. semiinvoluta* Zone layer represent the same event as the microspherules of the lower *Gl. cerroazulensis* Zone layer. In an effort to determine whether major element composition is a sufficient and conclusive criterion for differentiating between microtektite layers, we have analyzed the major element composition of microspherules from all three late Eocene stratigraphic layers. Our data were subjected to statistical analysis to determine major element compositional trends within and between the microspherule populations of the three microtektite layers. We present here the results of these analyses.

## METHODOLOGY

Major element chemical analyses were determined for this study using Princeton's electron microprobe. This microprobe consists of a 1968 ARL-EMX wavelength dispersive system (WDS) with a dual floppy disc 32K computer and software supplied by the manufacturer (Hollister *et al.*, 1984). The tektite glass standard used in these analyses was manufactured by Corning Glass and analyzed as a standard by the U.S. Geological Survey. For this study, two to four 50 second energy dispersive (EDS) analyses were made at different locations on a polished interior section of each microspherule. The results were normalized and averaged in order to obtain a representative analysis of each individual microspherule. The results shown in Table 1 and used throughout this report are of these averaged analyses. The analyses are given as weight percent oxides. FeO and $Fe_2O_3$ are plotted as cumulative FeO weight percent because the electron microprobe does not distinguish between $Fe^{2+}$ and $Fe^{3+}$. Sodium volatilization was checked for concurrent with random EDS analyses by using WDS at both 5 second and 20,000 count intervals. No significant sodium loss during the individual EDS analyses was apparent.

**Table 1**

**Major element composition of late Eocene microspherules. Note the abundance of crystal bearing microspherules in the lower *Gl. cerroazulensis* Zone layer.**

| specimen | no. of analyses averaged | $SiO_2$ | $Al_2O_3$ | FeO | MgO | CaO | $Na_2O$ | $K_2O$ | $TiO_2$ | MnO |
|---|---|---|---|---|---|---|---|---|---|---|
| a) The North American layer microtektites | | | | | | | | | | |
| Site RC9-58 (250 cm) microtektites | | | | | | | | | | |
| M2S20 | 3 | 73.82 | 15.17 | 4.45 | .76 | 1.06 | 1.01 | 2.99 | .73 | 0 |
| M2S21 | 3 | 67.09 | 16.41 | 5.89 | 3.08 | 2.54 | 1.14 | 1.94 | .76 | .12 |
| M2S22 | 3 | 78.16 | 12.63 | 2.61 | .77 | .97 | .95 | 3.08 | .61 | .22 |
| M2S23 | 3 | 64.70 | 17.55 | 6.22 | 2.74 | 2.43 | 1.46 | 3.69 | 1.07 | .16 |
| M2S24 | 3 | 63.52 | 17.75 | 6.24 | 3.26 | 2.64 | 1.88 | 3.68 | .97 | .07 |
| M2S25 | 4 | 69.24 | 16.52 | 5.38 | 1.97 | 1.64 | 1.25 | 3.06 | .94 | 0 |
| M2S27 | 3 | 72.97 | 13.97 | 4.16 | 1.37 | 2.00 | 1.26 | 3.51 | .69 | .07 |
| M2S28 | 2 | 75.75 | 14.13 | 3.85 | .74 | 1.27 | .93 | 2.82 | .68 | .11 |
| M2S29 | 3 | 71.49 | 15.17 | 4.34 | 1.54 | 1.69 | 1.07 | 3.90 | .76 | 0 |
| M2S30 | 3 | 68.17 | 17.69 | 6.10 | 1.35 | 1.43 | .87 | 3.04 | 1.08 | .22 |
| M2S34 | 2 | 66.46 | 17.27 | 5.64 | 3.08 | 2.81 | 1.12 | 2.64 | 1.01 | 0 |
| M2S35 | 2 | 79.67 | 11.24 | 3.08 | .46 | .99 | .78 | 3.31 | .51 | 0 |
| M2S38 | 3 | 78.43 | 12.54 | 3.09 | .33 | .77 | .94 | 3.30 | .50 | .09 |
| M2S39 | 2 | 72.75 | 15.34 | 5.17 | 1.20 | 1.32 | .70 | 2.41 | .86 | .31 |
| M2S40 | 3 | 68.53 | 15.85 | 5.53 | 2.58 | 2.60 | 1.01 | 2.78 | .85 | .23 |
| M2S41 | 3 | 75.36 | 14.16 | 4.27 | .68 | 1.06 | .82 | 2.96 | .65 | .06 |
| M2S42 | 3 | 78.57 | 12.16 | 3.17 | .41 | .70 | .92 | 3.19 | .78 | 0 |
| M2S43 | 4 | 76.64 | 12.90 | 3.71 | .94 | 1.21 | .93 | 2.85 | .76 | .06 |
| M2S44 | 3 | 80.16 | 11.55 | 2.41 | .43 | .54 | 1.10 | 3.03 | .66 | .07 |
| Bath Cliff, Barbados microtektites (from sample EO-9) | | | | | | | | | | |
| M4S1 | 3 | 81.54 | 11.30 | 2.70 | 0 | .34 | 1.23 | 2.36 | .46 | .07 |
| M4S4 | 3 | 79.26 | 12.16 | 2.97 | .53 | 1.11 | .81 | 2.59 | .54 | 0 |
| M4S5 | 3 | 78.76 | 12.37 | 2.94 | .32 | .27 | 1.32 | 3.16 | .74 | .12 |
| M4S8 | 2 | 76.28 | 13.47 | 4.37 | .96 | .48 | 1.27 | 2.46 | .72 | 0 |
| M4S9 | 2 | 79.30 | 12.19 | 2.22 | .44 | .62 | 1.25 | 3.27 | .71 | 0 |
| M4S10 | 3 | 82.03 | 10.69 | 2.50 | .42 | .42 | .82 | 2.42 | .43 | 0 |
| M4S11 | 3 | 79.04 | 12.42 | 3.32 | .50 | .40 | .91 | 2.63 | .71 | .06 |
| M4S12 | 2 | 78.32 | 11.30 | 4.01 | .59 | .77 | 1.15 | 3.29 | .60 | 0 |
| DSDP Site 94 15-4 (45-48 cm) microtektites | | | | | | | | | | |
| M5S13 | 3 | 84.16 | 8.15 | 2.13 | .60 | .80 | .84 | 1.91 | .56 | .12 |
| M5S14 | 2 | 77.64 | 13.29 | 2.97 | .66 | .76 | 1.06 | 2.81 | .60 | .18 |
| M5S15 | 2 | 74.83 | 13.06 | 3.47 | 1.36 | 1.60 | 1.68 | 3.00 | 1.03 | 0 |
| M5S16 | 3 | 73.85 | 14.08 | 4.47 | 1.26 | 1.46 | 1.48 | 2.79 | .62 | 0 |
| DSDP Site 94 15-3 (97-112 cm) microtektites | | | | | | | | | | |
| M5S24 | 2 | 66.93 | 15.22 | 5.77 | 1.87 | 2.62 | 3.04 | 3.56 | .95 | 0 |
| M5S25 | 2 | 77.66 | 13.12 | 3.30 | .44 | 1.13 | 1.13 | 2.65 | .47 | .12 |
| M5S26 | 2 | 73.38 | 12.72 | 5.88 | 1.23 | 1.87 | 1.29 | 2.92 | .48 | .25 |

### Table 1 — continued

| specimen | no. of analyses averaged | $SiO_2$ | $Al_2O_3$ | FeO | MgO | CaO | $Na_2O$ | $K_2O$ | $TiO_2$ | MnO |
|---|---|---|---|---|---|---|---|---|---|---|
| DSDP Site 612 21-5 microtektites | | | | | | | | | | |
| NJTEK1 | 3 | 73.12 | 15.22 | 4.59 | 1.23 | 0.65 | .64 | 3.62 | .90 | .09 |
| NJTEK2 | 4 | 72.97 | 15.09 | 5.00 | 1.16 | 0.76 | .38 | 3.68 | .92 | .04 |
| NJTEKA1 | 3 | 72.34 | 16.08 | 4.61 | 1.35 | .91 | .55 | 3.44 | .91 | .06 |
| NJTEKA2 | 4 | 82.93 | 10.52 | 2.06 | .56 | .61 | .55 | 2.39 | .30 | .05 |
| NJTEKA3 | 4 | 73.54 | 14.49 | 4.61 | .95 | 1.12 | 1.42 | 2.83 | .96 | .10 |
| NJTEKA5 | 3 | 74.48 | 14.41 | 4.45 | 1.09 | .95 | .78 | 2.90 | .87 | .06 |
| NJTEKA6 | 3 | 74.30 | 14.45 | 4.54 | 1.01 | 1.05 | .77 | 3.09 | .80 | 0 |
| NJTEKA7 | 3 | 73.45 | 15.17 | 4.57 | 1.22 | .99 | 1.05 | 2.85 | .71 | 0 |
| NJTEKA8 | 3 | 74.44 | 14.96 | 3.31 | .62 | .74 | 1.35 | 4.03 | .54 | 0 |
| NJTEKA10 | 4 | 72.26 | 15.58 | 4.84 | 1.28 | .92 | .69 | 3.60 | .84 | .05 |
| NJTEKA11 | 3 | 68.62 | 15.28 | 5.12 | 1.78 | 2.97 | 2.39 | 3.16 | .61 | 0 |
| NJTEKA12 | 3 | 75.28 | 13.91 | 4.19 | 1.02 | .99 | .78 | 3.02 | .71 | .1 |
| NJTEKA13 | 3 | 71.68 | 14.61 | 4.84 | 1.66 | 2.08 | 1.50 | 2.78 | .85 | 0 |
| NJTEKA14 | 3 | 71.36 | 15.44 | 5.18 | 1.15 | 1.13 | 1.47 | 2.95 | .87 | .14 |
| NJTEKA15 | 3 | 79.29 | 11.89 | 3.71 | .93 | .50 | .17 | 2.49 | .84 | .20 |
| NJTEKA16 | 3 | 73.24 | 14.99 | 4.65 | 1.39 | .66 | .60 | 3.49 | .97 | 0 |
| NJTEKA17 | 3 | 74.87 | 14.42 | 3.89 | .99 | 1.09 | .93 | 3.07 | .89 | .06 |
| NJTEKA18 | 2 | 72.72 | 15.10 | 4.18 | 1.13 | 1.21 | 1.67 | 3.04 | .83 | .14 |
| NJTEKA19 | 2 | 73.79 | 14.11 | 4.62 | .99 | 1.14 | 1.27 | 2.93 | .87 | .27 |
| NJTEKA20 | 2 | 74.94 | 14.24 | 4.80 | .95 | .90 | 1.17 | 2.77 | .85 | .12 |
| NJTEKA21 | 2 | 73.37 | 14.47 | 5.00 | 1.14 | .74 | .57 | 3.61 | 1.01 | .10 |
| b) The microspherules of the lower *Gl. cerroazulensis* Zone layer | | | | | | | | | | |
| RC9-58 (280 cm) microtektites and associated crystal-bearing microspherules | | | | | | | | | | |
| M2S1* | 4 | 59.47 | 6.99 | 12.76 | 10.22 | 7.09 | 1.72 | 1.71 | .31 | .24 |
| M2S2* | 2 | 68.03 | 9.18 | 11.17 | 3.04 | 2.72 | 1.72 | 3.61 | .41 | .14 |
| M2S3* | 3 | 59.35 | 7.04 | 11.43 | 7.72 | 11.13 | 1.01 | 1.73 | .34 | .26 |
| M2S6* | 2 | 64.93 | 11.61 | 10.09 | 2.16 | 6.70 | 1.18 | 2.67 | .48 | .17 |
| M2S7 | 3 | 58.06 | 4.83 | 13.01 | 13.87 | 7.21 | 1.14 | 1.57 | .23 | .06 |
| M2S9* | 3 | 62.82 | 12.02 | 10.01 | 2.68 | 6.73 | 1.83 | 3.41 | .51 | 0 |
| M2S10 | 3 | 63.16 | 8.19 | 11.11 | 4.89 | 9.45 | 1.04 | 1.66 | .41 | .25 |
| M2S11 | 4 | 58.50 | 6.96 | 12.35 | 13.46 | 5.49 | 1.11 | 1.72 | .16 | .23 |
| M2S12 | 3 | 63.48 | 9.60 | 9.59 | 9.01 | 3.66 | 1.31 | 2.69 | .60 | .07 |
| M2S13* | 3 | 62.74 | 7.56 | 8.21 | 8.40 | 9.93 | .89 | 1.71 | .41 | .15 |
| M2S14 | 3 | 62.39 | 6.09 | 8.36 | 11.28 | 9.20 | .98 | 1.24 | .29 | .18 |
| M2S15* | 3 | 65.81 | 9.03 | 8.94 | 3.10 | 8.79 | 1.30 | 2.56 | .47 | 0 |
| M2S16 | 4 | 67.28 | 6.01 | 5.92 | 8.47 | 9.60 | .67 | 1.54 | .34 | 0 |
| M2S17 | 2 | 63.08 | 5.66 | 13.08 | 9.70 | 3.79 | 1.59 | 2.62 | .18 | .32 |
| M2S18* | 3 | 64.25 | 11.52 | 6.75 | 3.99 | 7.00 | 1.71 | 4.25 | .44 | .09 |
| M2S19* | 3 | 56.65 | 4.84 | 8.19 | 12.49 | 14.66 | 1.08 | 1.74 | .21 | .13 |

*crystal-bearing microspherule

### Table 1 — continued

| specimen | no. of analyses averaged | $SiO_2$ | $Al_2O_3$ | FeO | MgO | CaO | $Na_2O$ | $K_2O$ | $TiO_2$ | MnO |
|---|---|---|---|---|---|---|---|---|---|---|
| DSDP Site 315A 10-6 (32 cm) microtektites and related microspherules | | | | | | | | | | |
| M3S4 | 2 | 59.03 | 4.34 | 5.19 | 12.40 | 16.64 | .61 | 1.46 | .31 | 0 |
| M3S5 | 3 | 62.83 | 5.56 | 6.57 | 11.36 | 11.36 | .61 | 1.36 | .35 | 0 |
| M3S7* | 3 | 64.04 | 7.67 | 10.36 | 7.11 | 7.68 | .98 | 1.78 | .28 | .06 |
| M3S9* | 3 | 65.56 | 6.61 | 9.29 | 5.86 | 10.58 | .64 | 1.39 | .07 | 0 |
| DSDP Site 69A, 9-5 (12-45 cm) microtektites and related microspherules | | | | | | | | | | |
| M3S14* | 3 | 61.64 | 4.35 | 12.28 | 14.11 | 5.23 | .38 | 1.62 | .20 | .20 |
| M3S15* | 3 | 61.97 | 6.58 | 14.66 | 7.06 | 6.72 | .53 | 1.91 | .27 | .23 |
| M3S17 | 3 | 61.22 | 4.89 | 11.24 | 11.17 | 8.39 | .79 | 1.97 | .22 | .13 |
| M3S18* | 2 | 63.76 | 7.27 | 10.93 | 4.78 | 7.02 | 1.50 | 3.91 | .58 | .33 |
| M3S22 | 3 | 61.46 | 6.12 | 12.45 | 10.82 | 5.62 | .83 | 2.21 | .38 | 0 |
| DSDP Site 462A 36-1 (144-146 cm) microtektites | | | | | | | | | | |
| M5S5 | 3 | 64.38 | 11.38 | 6.77 | 5.46 | 3.70 | 3.23 | 4.24 | .78 | .06 |
| M5S5.5 | 2 | 63.55 | 11.26 | 7.34 | 5.49 | 3.94 | 3.38 | 4.23 | .57 | .24 |
| M5S6 | 2 | 67.32 | 6.70 | 4.64 | 7.78 | 10.42 | .60 | 2.04 | .29 | .22 |
| M5S7 | 3 | 65.66 | 10.34 | 7.66 | 5.32 | 3.01 | 3.03 | 4.31 | .58 | 0 |
| M5S11 | 3 | 60.93 | 7.07 | 10.55 | 4.92 | 12.75 | 1.30 | 2.10 | .13 | .24 |
| c) Microspherules of the *G. semiinvoluta* Zone microtektite layer | | | | | | | | | | |
| DSDP Site 292 38-2 (1-21 cm) microtektites | | | | | | | | | | |
| M1S1 | 3 | 67.73 | 6.40 | 3.34 | 7.71 | 12.26 | .33 | 1.84 | .31 | 0 |
| M1S2 | 3 | 68.33 | 5.34 | 4.07 | 8.17 | 11.37 | .56 | 1.82 | .24 | .06 |
| M1S3 | 3 | 65.51 | 5.60 | 9.36 | 7.44 | 6.48 | 1.92 | 3.13 | .39 | .17 |
| M1S4a | 3 | 70.36 | 6.44 | 6.72 | 6.75 | 6.55 | .63 | 2.00 | .36 | .18 |
| M1S4b | 2 | 58.73 | 3.99 | 3.59 | 13.06 | 19.19 | .19 | .98 | .29 | 0 |
| M1S10 | 3 | 66.12 | 5.34 | 4.32 | 9.74 | 11.56 | .63 | 1.92 | .41 | 0 |
| DSDP Site 216, 16-2 (~ 1-5 cm) microtektites and related microspherules | | | | | | | | | | |
| M5S28 | 3 | 70.11 | 8.00 | 9.32 | 2.10 | 4.62 | 1.53 | 3.19 | .77 | .16 |
| M5S34 | 2 | 60.06 | 4.49 | 3.30 | 11.58 | 18.02 | .50 | 1.75 | .28 | 0 |
| M5S39 | 3 | 70.13 | 8.69 | 1.56 | 4.71 | 9.36 | 1.00 | 4.30 | .25 | 0 |
| M5S40 | 3 | 64.21 | 5.03 | 2.74 | 9.25 | 15.50 | .55 | 2.17 | .40 | .07 |
| M5S42 | 2 | 74.74 | 15.77 | 2.97 | 1.09 | .97 | .56 | 2.88 | .98 | 0 |
| M5S43 | 3 | 69.72 | 6.86 | 3.50 | 6.72 | 10.05 | .85 | 1.76 | .40 | .07 |
| M5S44 | 3 | 74.17 | 10.85 | 5.27 | 1.75 | 3.55 | .60 | 3.39 | .42 | 0 |
| M5S45 | 3 | 68.57 | 5.21 | 8.37 | 7.99 | 6.88 | .91 | 1.79 | .26 | .08 |
| M6S4 | 2 | 63.12 | 5.92 | 5.32 | 8.71 | 12.35 | 1.20 | 2.92 | .28 | .20 |
| M6S5 | 3 | 59.19 | 4.78 | 7.46 | 11.05 | 15.08 | .64 | 1.49 | .23 | .07 |
| M6S6 | 2 | 58.57 | 4.68 | 3.52 | 11.16 | 18.74 | .48 | 2.61 | .26 | 0 |

*crystal-bearing microspherule

Table 1 — continued

| specimen | no. of analyses averaged | $SiO_2$ | $Al_2O_3$ | FeO | MgO | CaO | $Na_2O$ | $K_2O$ | $TiO_2$ | MnO |
|---|---|---|---|---|---|---|---|---|---|---|
| M6S7 | 2 | 58.43 | 5.98 | 4.49 | 9.94 | 19.12 | .31 | 1.02 | .45 | .28 |
| M6S8 | 3 | 73.42 | 5.99 | 3.17 | 5.99 | 9.09 | .51 | 1.66 | .14 | 0 |
| M6S9* | 3 | 67.59 | 7.55 | 9.87 | 4.78 | 6.23 | 1.10 | 2.31 | .44 | .08 |
| M6S12 | 3 | 70.08 | 4.64 | 2.46 | 7.55 | 12.51 | .28 | 1.99 | .38 | .12 |
| M6S13 | 2 | 65.93 | 5.51 | 9.05 | 8.48 | 7.61 | .92 | 2.00 | .28 | .25 |
| M6S13.5 | 1 | 73.82 | 7.07 | 7.35 | 2.56 | 4.72 | 1.08 | 2.64 | .50 | 0 |
| M6S16 | 3 | 60.95 | 4.95 | 3.34 | 10.46 | 17.32 | .42 | 2.18 | .30 | .08 |
| M6S17 | 2 | 78.76 | 15.89 | .76 | .14 | .12 | 0 | 3.48 | .88 | 0 |
| M6S18 | 4 | 69.06 | 7.31 | 7.53 | 5.48 | 3.91 | 2.34 | 9.73 | .46 | 0 |
| M6S19 | 2 | 61.86 | 10.30 | 10.09 | 9.40 | 5.26 | .99 | 1.74 | .56 | .09 |
| M6S19.5 | 3 | 70.34 | 13.88 | 4.49 | 1.20 | 4.94 | 1.04 | 2.96 | .62 | .10 |
| M6S25 | 3 | 66.06 | 6.59 | 11.79 | 5.93 | 6.09 | .96 | 2.07 | .47 | 0 |
| M6S26* | 3 | 63.53 | 6.51 | 10.72 | 7.51 | 5.85 | 1.61 | 3.92 | .18 | .17 |
| d) *G. semiinvoluta* Zone possible microtektites of Molino de Cobo, Spain, sample MC-4 | | | | | | | | | | |
| MC4A2[1] | 5 | 34.52 | 20.65 | 14.82 | 11.81 | 14.69 | 0 | 2.41 | .75 | .34 |
| MC4B3 | 3 | 43.10 | 29.04 | 15.39 | .71 | 5.78 | 1.58 | 3.21 | 1.13 | .06 |
| MC4B5 | 3 | 52.96 | 31.43 | 4.05 | 1.52 | 2.11 | .87 | 5.91 | .91 | .16 |
| MC4B6[1] | 5 | 41.27 | 28.58 | 17.94 | 1.92 | 6.02 | .07 | 3.15 | .77 | .25 |
| MC4B8[1] | 4 | 50.88 | 16.03 | 24.41 | 1.19 | 3.92 | .79 | 1.82 | .93 | .51 |
| MC4B9[2] | 3 | 29.39 | 48.37 | 12.04 | 1.41 | 4.87 | .17 | 1.70 | 1.96 | 0 |
| MC4B9B | 3 | 50.82 | 28.98 | 8.40 | 1.28 | 3.44 | .73 | 5.28 | 1.07 | 0 |
| MC4B12 | 3 | 25.69 | 8.92 | 3.29 | 2.57 | 33.34 | .13 | 1.31 | .73 | 24.02 |
| MC4B12 | inclusion | 99.80 | 0 | 0 | 0 | 0 | 0 | 0 | 0 | 0.20 |
| MC41 | 2 | 51.39 | 30.16 | 7.22 | 2.22 | 5.15 | .39 | 2.50 | .98 | 0 |

*crystal-bearing microspherule

[1] highly variable sample

[2] fused to MC4B9B

The EDS determined compositional analyses were subjected to statistical R-mode factor analysis in order to determine relationships between elements in the different late Eocene microtektite layers. Because MnO is present in all populations of analyzed microspherules in concentrations too low for statistically significant energy-dispersive microprobe analysis, MnO concentrations were excluded from this multivariate statistical analysis. The microspherule compositional analyses were first normalized so that all elemental variables ranged from 0 to 1. The factor analysis package BMDP4M was used. The first two factors determined by principle components analysis and followed by Varimax rotation account for 77.99% of the variance in major element compositional trends of late Eocene microtektites and partially crystalline spherules.

In order to determine relationships between individual microspherules, statistical Q-mode factor analysis was applied to the same compositional data. Again the compositional analyses were first normalized so that all elemental variables ranged from 0 to 1. The BMDP factor analysis package was again used. Principle components analysis followed by Varimax rotation provided three factors which account for 96.84% of the compositional variation between individual late Eocene microspherules. For interpretive and graphic display purposes, these three statistical Q-mode factors were obliquely rotated to the extent that all factor scores determined were greater than or equal to zero.

## RESULTS

### North American Microtektite layer: *Globorotalia cerroazulensis* Zone

Microtektites from the upper *Gl. cerroazulensis* Zone layer have been identified as part of the North American tektite strewnfield (Glass *et al.*, 1973; NgO *et al.*, 1985). For this study, microtektites from this layer were analyzed from Caribbean piston core RC9-58 at 250 cm, from Caribbean DSDP Site 94 in core sections 15-3 and 15-4, from sample EO-9 of the Bath Cliff section of Barbados, and from Atlantic DSDP Site 612 in core-section 21-5 (Fig. 1). EDS data shows microtektites of this North American horizon to contain generally higher concentrations of $SiO_2$, $Al_2O_3$, and $TiO_2$ than the microspherules of the two older late Eocene events. Furthermore, microtektites of the upper *Gl. cerroazulensis* Zone horizon exhibit generally lower values of CaO and MgO than $SiO_2$-equivalent microspherules of the two earlier late Eocene events (Fig. 2, Table 1). Previous workers have observed that 91% to 95% of the microspherules of the North American horizon are glassy microtektites; the remainder are cryptocrystalline and crystal-bearing microspherules (Glass *et al.*, 1985). All of the North American horizon microspherules observed for this report are glassy microtektites (Table 1). At DSDP Site 612, the microtektites of this horizon are associated with large (up to 2 cm long) fragments of compositionally identical glass containing partially resorbed crystals and abundant elongate bubbles.

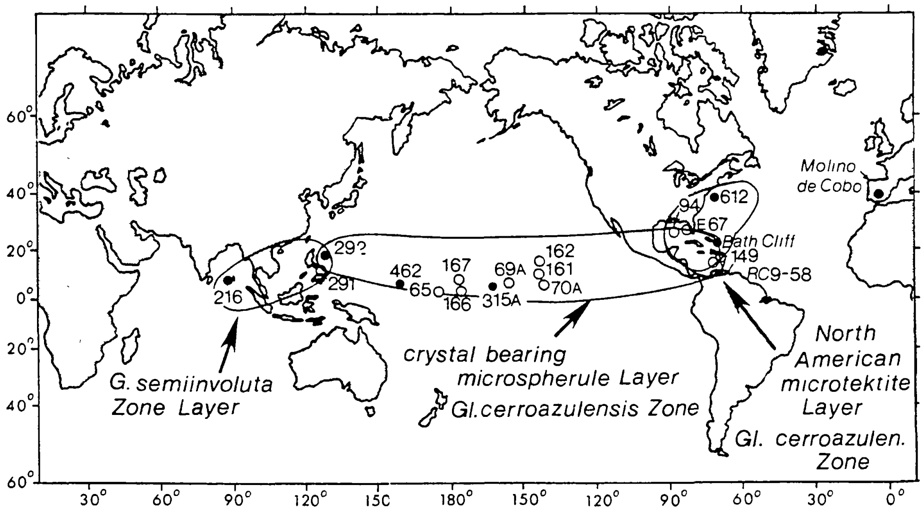

**Fig. 1** Geographic location of sampled sites.

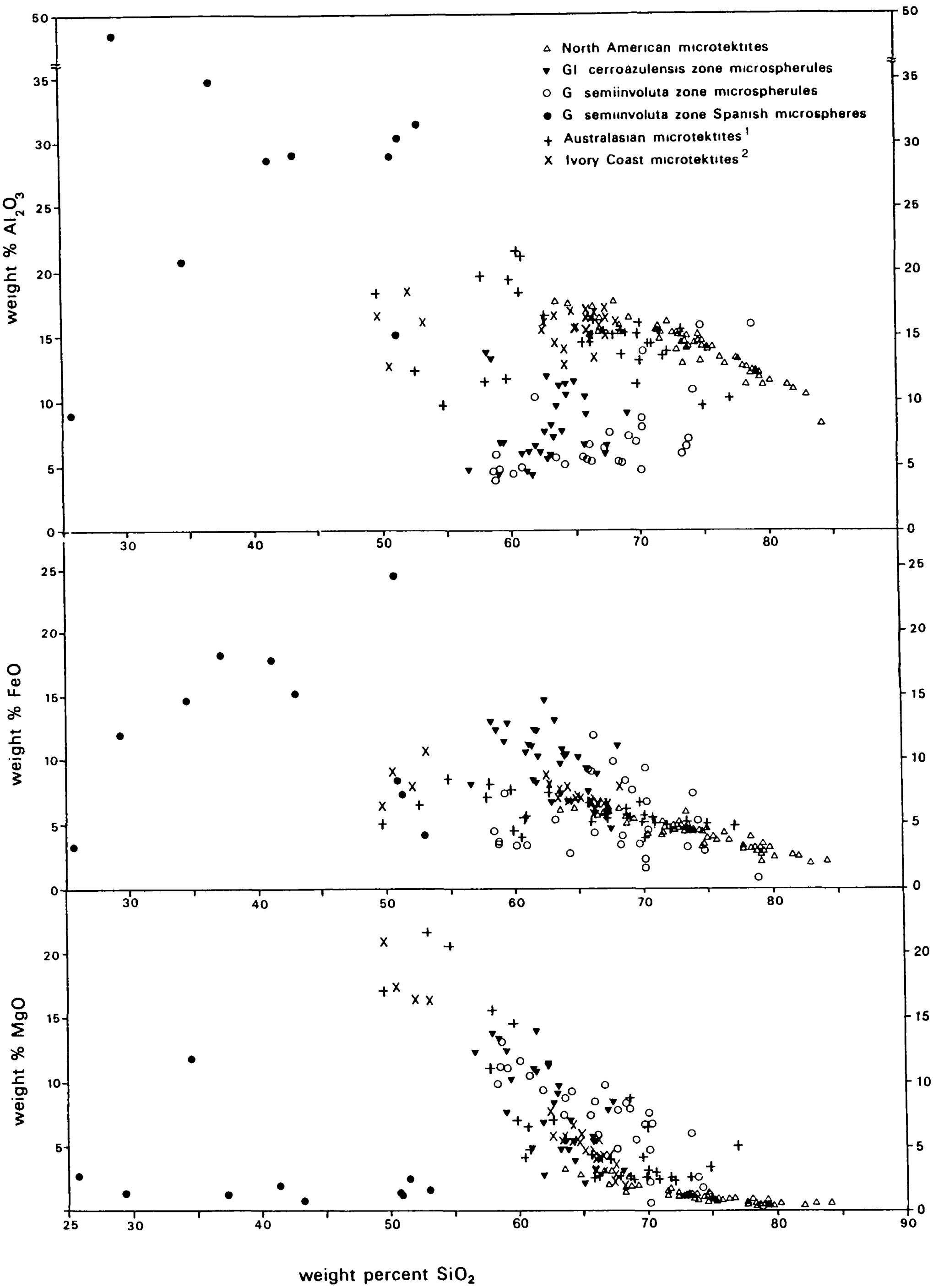

1 Data from Cassidy et al, 1969

2 Data from Glass, 1969

Fig. 2 Major oxide vs. $SiO_2$ content for microspherules of three late Eocene horizons and the Australasian and Ivory Coast microtektite strewnfields.

1987Metic..22...61D

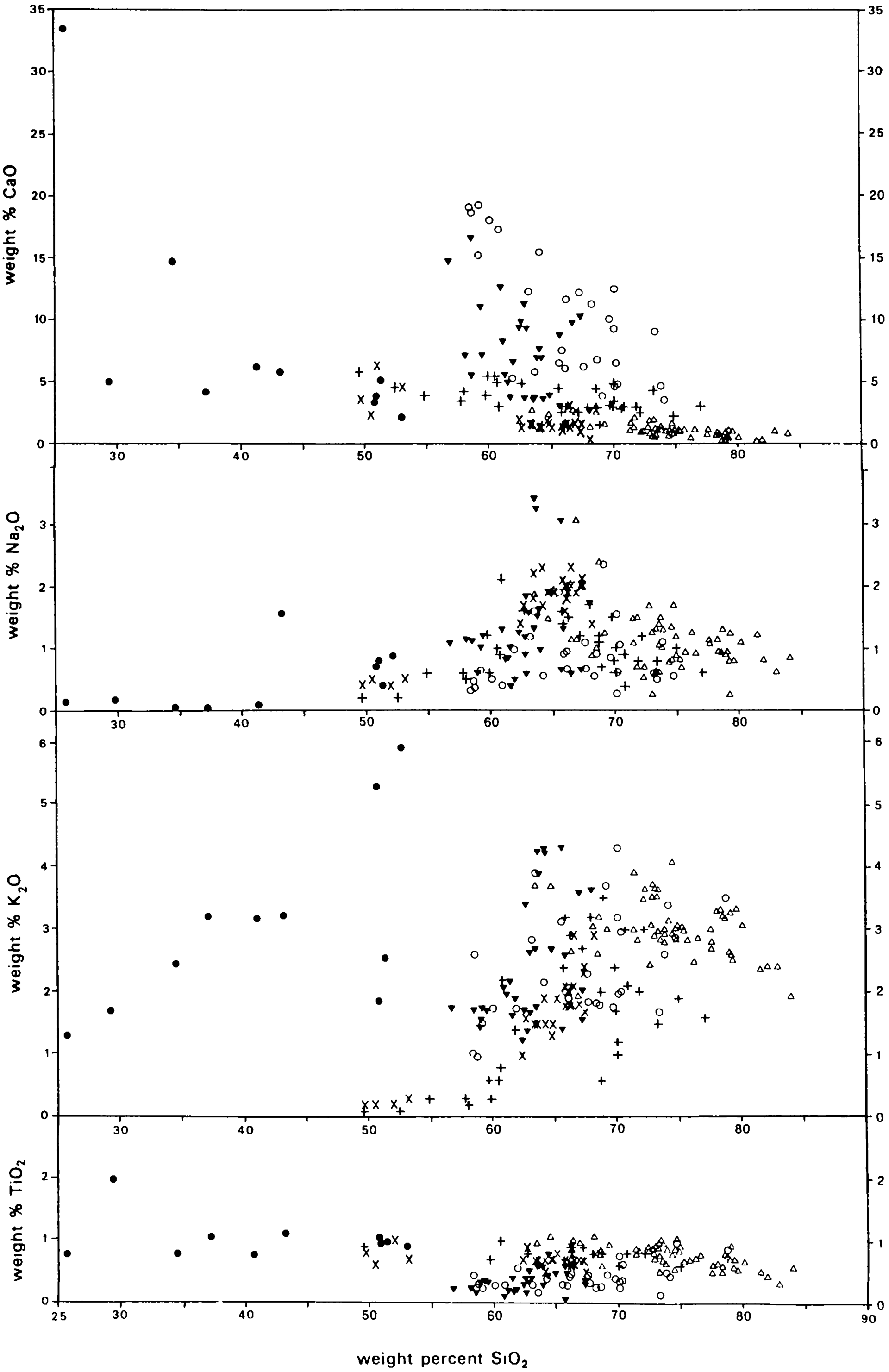

Fig. 2 continued

## Crystal-bearing Microspherules: *Globorotalia cerroazulensis* Zone

Microspherules of the crystal-bearing microspherule layer were originally discovered by Glass and coworkers (John and Glass, 1974). These earlier workers assigned these microspherules to the North American tektite strewnfield (John and Glass, 1974; Glass *et al.*, 1979, 1982; Ganapathy, 1982; Glass, 1984) but now recognize them as representative of an older layer (Glass *et al.*, 1985). This lower *Gl. cerroazulensis* Zone horizon includes both glassy microspherules (microtektites) and partially crystalline microspherules. Both glassy and partially crystalline microspherules of the lower *Gl. cerroazulensis* Zone horizon were studied from Caribbean piston core RC9-58 at 280 cm, and the mid-Pacific DSDP Site 69A in core-section 9-5 (Fig. 1).

According to Glass and coworkers (Glass *et al.*, 1985), there are two types of partially crystalline microspherules in this layer. The first type is characterized by microlites or crystallites imbedded in a glassy matrix whereas the second type is characterized by an almost completely cryptocrystalline texture and very little glassy matrix. Glass and coworkers (Glass *et al.*, 1985) generally refer to the former type as cpx spherules and the latter type as cryptocrystalline spherules. Because clinopyroxene is the major crystalline phase in both types of partially crystalline microspherules, this report refers to the former as crystal-bearing microspherules and the latter as cryptocrystalline microspherules. According to previous workers, 41% to 72% of the microspherules of the lower *Gl. cerroazulensis* Zone layer are crystal-bearing microspherules, 20% to 57% are cryptocrystalline microspherules, and the remaining 2% to 8% are glassy microtektites (Glass *et al.*, 1985). These findings are consistent with those of this report (Tables 1, 2).

**Table 2**
**Average composition of lower *Gl. cerroazulensis* Zone noncrystal-bearing microspherules and related crystal-bearing microspherules**

| | $SiO_2$ | $Al_2O_3$ | FeO | MgO | CaO | $Na_2O$ | $K_2O$ | $TiO_2$ | no. of microspherules averaged |
|---|---|---|---|---|---|---|---|---|---|
| crystal bearing microspherules | 62.93 | 8.02 | 9.52 | 6.63 | 8.00 | 1.18 | 2.43 | .32 | 14 |
| noncrystal-bearing microspherules | 62.65 | 7.20 | 9.82 | 9.08 | 7.76 | 1.39 | 2.32 | .39 | 16 |

The crystal-bearing microspherules of this layer sometimes include prismatic, hopper, chain, feathery, or dendritic shaped voids which presumably once contained crystalline material. Glass and coworkers (Glass *et al.*, 1985) have suggested that the now missing phases are probably Mg-rich olivine and Fe-rich pyroxene. The possible removal of some olivine from the crystal-bearing microspherule population is consistent with observed slight differences in mean composition between the studied population of crystal-bearing microspherules and the analyzed population of noncrystal-bearing microspherules from this layer (Table 2). Despite the small differences in mean composition between the studied population of noncrystalline microtektites and the analyzed population of crystal-bearing microspherules, individual noncrystalline microtektites and individual crystal-bearing microspherules of this layer commonly exhibit major element compositional overlap (Tables 1, 2). Both partially crystalline microspherules and glassy microtektites of this crystal-bearing microspherule layer contain considerably lower values of $Al_2O_3$ and $TiO_2$ and generally higher concentrations of CaO, FeO, and MgO than the silica-equivalent microtektites of the stratigraphically younger North American horizon (Fig. 2, Table 1).

### *Globigerapsis semiinvoluta* Zone microspherule layer

Microspherules of the oldest of these three late Eocene microtektite events have been discovered at western Pacific Site 292 in core-section 38-2 and at Indian Ocean DSDP Site 216 in core-section 16-2 (Keller *et al.*, 1983, 1987) (Fig. 1). The microspherules of this oldest known late Eocene layer at Sites 292 and 216 often show higher CaO concentrations and lower values of $Al_2O_3$ and $Na_2O$ than silica equivalent microspherules of the two younger late Eocene horizons (Fig. 2, Table 1). The presence of a short hiatus at the microtektite layer in Indian Ocean DSDP Site 216, core-section 16-2 prevents definite stratigraphic assignment of this layer. However, Keller *et al.* (1987) conclude that stratigraphic and petrographic characteristics suggest that it is probably the *G. semiinvoluta* Zone event. This observation is consistent with the *G. semiinvoluta* Zone microspherule compositional trends and geographic proximity to DSDP Site 292, core-section 38-2 (Fig. 1, Table 1).

Low abundances of crystal-bearing microspherules occur at DSDP Sites 292 and 216. Glass *et al.* observe that 12% to 18% of the microspherules at these sites are crystal-bearing (1985). This observation is consistent with this report (Table 1). Sixty-four percent to 65% of the microspherules at this site are described as cryptocrystalline by Glass and coworkers, who described the remainder as glassy microtektites (Glass *et al.*, 1985). When this petrographic data of Glass *et al.* is plotted on a ternary diagram, it becomes evident that the microspherule population of DSDP Site 216 petrographically resembles that of DSDP Site 292 (Fig. 3). It also becomes evident that the three stratigraphic microspherule horizons are clearly distinguishable based on the petrographic criteria of Glass *et al.* (1985).

*Globigerapsis semiinvoluta* Zone microspheres have been discovered in the Molino de Cobo section of southern Spain. These glassy micro-objects closely resemble microtektites in shape and surface morphology and occur at the same stratigraphic level as the *G. semiinvoluta* Zone microspherules of DSDP Sites 292, 38-2 and 216, 16-2 (Keller *et al.*, 1987). The Spanish microspheres occasionally contain inclusions of pure $SiO_2$ but are sometimes compositionally highly variable and exhibit very little major element compositional overlap with other late Eocene microtektites or crystal-bearing microspherules. The *G. semiinvoluta* Zone micro-objects of Molino de Cobo typically contain low concentrations of $SiO_2$ and high concentrations of $Al_2O_3$ relative to other analyzed late Eocene microspheres (Fig. 2, Table 1).

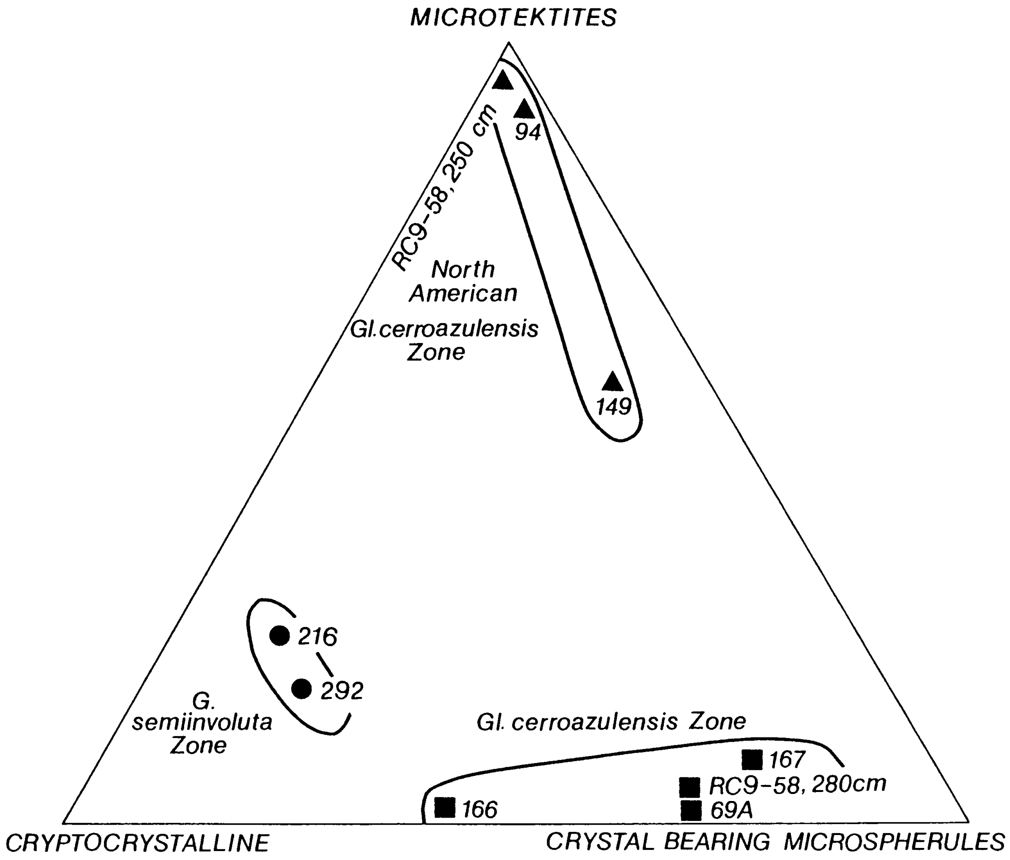

**Fig. 3 Ternary diagram of microspherule types: microtektites, cryptocrystalline microspherules, and crystal-bearing microspherules (data from Glass *et al.*, 1985).**

## STATISTICAL ANALYSIS

When other major elements are plotted against silica, as in Figure 1, the microspherule populations of the lower *Gl. cerroazulensis* Zone horizon and the Pacific and Indian Ocean *G. semiinvoluta* Zone horizon exhibit considerable major element compositional overlap. Based in part on this compositional overlap, previous workers concluded that the two layers represent the same event (Glass *et al.*, 1985). In order to effectively address this conclusion, it becomes useful to simultaneously assess the relationships between all major elements of the microtektite populations in question. In this study we quantitatively clarify compositional differences and similarities between microtektites and related microspherules of the different late Eocene horizons by examining the compositional data using R-mode and Q-mode factor analyses. In the absence of definitive recognition of the Molino de Cobo *G. semiinvoluta* Zone microspheres as microtektites or related microspherules, they are excluded from this R-mode and Q-mode factor analysis of late Eocene microtektites and related crystal-bearing glassy microspherules.

## R-mode Factor Analysis:

R-mode factor analysis determines relationships between variables, i.e. the degree of covariance among major oxides. Primary relationships between major elements in microspherules of all three layers were studied using R-mode analysis. It was found that two R-mode factors explain 77.99% of the variance in major element compositional trends. The first factor explains 58.33% of the total variance, is consistent with Bowen's reaction series, and assigns strong positive factor loadings to $Al_2O_3$, $TiO_2$, $K_2O$, and $SiO_2$ and a moderate positive factor loading to $Na_2O$. Additionally, the first factor is strongly negatively loaded for CaO and MgO and moderately negatively loaded for FeO. The second factor explains 19.66% of the variance. This second factor shows $Na_2O$ to be strongly positively correlated to FeO, strongly negatively correlated to $SiO_2$, and moderately positively correlated to MgO and $K_2O$ in some of the samples (Table 3).

**Table 3**
**Rotated R-mode factor loadings**

| Variable | Factor 1 | Factor 2 |
|---|---|---|
| MgO | −0.892 | 0.312 |
| $Al_2O_3$ | 0.903 | −0.126 |
| FeO | −0.395 | 0.737 |
| $TiO_2$ | 0.841 | −0.078 |
| $SiO_2$ | 0.678 | −0.617 |
| CaO | −0.857 | 0.079 |
| $K_2O$ | 0.812 | 0.266 |
| $Na_2O$ | 0.418 | 0.785 |

Microtektites of the North American horizon exhibit generally positive values of factor 1 and negative values of factor 2 (Fig. 4). This indicates that microtektites of this horizon contain generally high concentrations of $SiO_2$, $Al_2O_3$, $TiO_2$, and $K_2O$ and relatively low concentrations of MgO and CaO. The compositional trends displayed by the microtektites of this horizon appear to parallel trends displayed by granitic rocks.

Microspherules of the lower *Gl. cerroazulensis* Zone horizon consistently exhibit positive values of factor 2 and generally exhibit negative values of factor 1 (Fig. 4). This indicates that the microspherules of this widespread late Eocene horizon contain relatively high concentrations of FeO, MgO, CaO, and $Na_2O$ and relatively low concentrations of $SiO_2$, $Al_2O_3$, and $TiO_2$. There is no overlap in compositional trends between these microspherules and the North American microtektites.

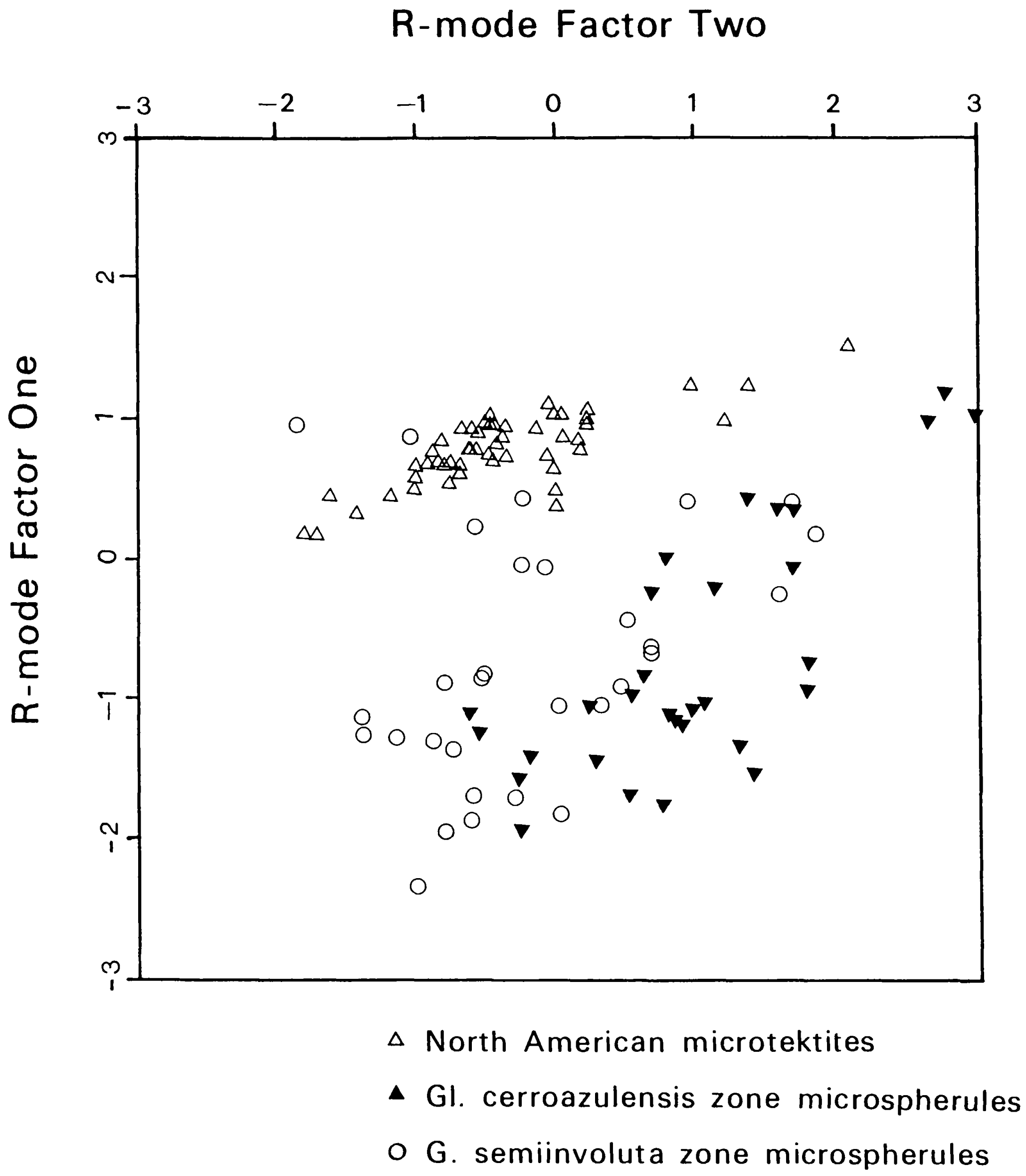

**Fig. 4** R-mode factor results. R-mode factors 1 and 2 represent statistical relationships between major elements. For R-mode factor loadings see Table 3.

Microspherules of the lowermost late Eocene horizon (*G. semiinvoluta* Zone) exhibit predominantly negative values of both R-mode factor 1 and R-mode factor 2, indicating the common presence of microspherules that contain high concentrations of CaO and low concentrations of $Na_2O$ and $Al_2O_3$ relative to microspherules of the other two late Eocene layers. However, individual microspherules from this horizon also commonly exhibit both negative and positive values of both factor 1 and factor 2 (Fig. 4). Microspherules of the *G. semiinvoluta* Zone horizon overlap the compositional trends exhibited by both the North American microtektites and the lower *Gl. cerroazulensis* Zone microspherules. Hence, major elements within microspherules of this oldest known late Eocene horizon show a much lower degree of covariance than major elements within microspherules of the two younger horizons. Based on R-mode factor analysis, microspherule populations from this *G. semiinvoluta* Zone layer are distinguishable from those of the other two layers both by this low degree of covariance and by the common presence of the high CaO, low $Na_2O$ microspherules.

## Q-mode Factor Analysis:

Q-mode factor analysis indicates relationships between samples, i.e. individual microtektites, unlike R-mode factor analysis which indicates relationships between variables. Compositional relationships between individual microtektites and related crystal bearing microspherules were therefore clarified using Q-mode factor analysis. Using this technique, three statistical factors account for 96.84 percent of the compositional variance between individual microspherules. When the resulting values for the individual microspherules are plotted against their hypothetical endmembers (factors) on a ternary diagram, it becomes evident that each factor is dominated by the microspherules of a different late Eocene microtektite horizon.

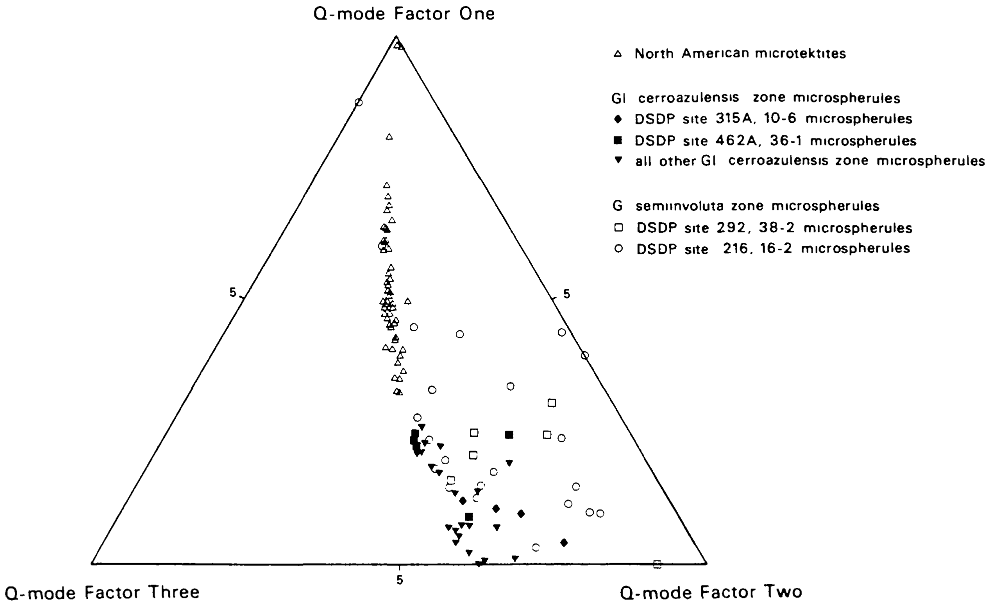

**Fig. 5** **Ternary diagram of Q-mode results. Note that each Q-mode factor is dominated by the microspherules of a different late Eocene layer. Compare to Figure 3.**

The North American microtektites dominate factor one (Fig. 5). Factor one represents a hypothetical endmember high in $SiO_2$, $Al_2O_3$, and $TiO_2$ and low in MgO, CaO, and FeO, as is consistent with our R-mode results. Factor two is dominated by the microspherules of the *G. semiinvoluta* Zone layer (Fig. 5). Factor two represents an endmember relatively enriched in CaO and MgO and relatively impoverished in $SiO_2$, $TiO_2$, $Al_2O_3$, FeO, and $Na_2O$, again consistent with our R-mode results. The lower *Gl. cerroazulensis* Zone horizon dominates factor three (Fig. 5). Factor three represents a hypothetical endmember relatively enriched in MgO, FeO, and $Na_2O$, low in $SiO_2$ and $TiO_2$, and with an $Al_2O_3$ composition intermediate between the other two groups. Addition of small amounts of a Mg-rich olivine or Fe-rich clinopyroxene phase to lower *Gl. cerroazulensis* Zone microspherules with missing phases would slightly increase the MgO or FeO values determined for those microspherules (Tables 1, 2).

Our Q-mode analysis indicates that the North American microtektite population appears to follow well-defined trends, whereas the microspherule population of the lower *Gl. cerroazulensis* Zone layer is less homogeneous, and the microspherule population of the *G. semiinvoluta* Zone horizon is highly heterogeneous (Fig. 5). These results are consistent with the trends observed in our Harker diagrams (Fig. 2). Unlike the Harker diagrams, the Q-mode analysis maximizes differences and similarities between individual microspherules by recognizing all major elements in each microspherule simultaneously.

Individual microspherules of the *G. semiinvoluta* Zone layer often exhibit major element compositions similar to those of the lower *Gl. cerroazulensis* Zone layer and occasionally exhibit major element compositions similar to those of the North American layer. Nevertheless, compositional trends of microspherule populations indicate that the three late Eocene microtektite layers stratigraphically determined by Keller *et al.* (1987) can be distinguished on the basis of major element compositional endmembers and populational variability (Figs. 4, 5).

Stratigraphically, it is not unequivocally clear to which layer to assign the microspherules of mid-Pacific DSDP Sites 315A, 10-6 and 462A, 36-1 (Keller *et al.*, 1987). Based on compositional properties and on geographic proximity to known occurrences, these microspherules can be provisionally assigned to the lower *Gl. cerroazulensis* Zone layer (Figs. 1, 5, Table 1). The microspherules discovered by Glass at DSDP Site 292 in core-section 36-2 have also been assigned by Keller and coworkers (Keller *et al.*, 1987) to the lower *Gl. cerroazulensis* Zone layer based on stratigraphic relationships. Glass and coworkers, however, consider these microspherules to be reworked from the underlying micro-spherule layer assigned by Keller *et al.* a *G. semiinvoluta* Zone biostratigraphic age (Keller *et al.*, 1983, 1986, 1987; Glass, 1984; Glass *et al.*, 1985). The few published analyses of Site 292 core-section 36-2 microspherules (Glass *et al.*, 1985) exhibit compositional trends of higher FeO and lower CaO concentrations than those of the Site 292, core 38-2 occurrence (Keller *et al.*, 1984, this report). This is consistent with the trends exhibited by our multivariate analysis and seems to suggest that the Site 292 core-section 36-2 microspherules belong to the lower *Gl. cedrroazulensis* Zone layer and are not reworked from the *G. semiinvoluta* Zone layer. Based on compositional properties and geographic proximity, the microspherules of Indian Ocean DSDP Site 216, 16-2, are assigned to the *G. semiinvoluta* Zone microspherule layer first discovered in western Pacific DSDP Site 292, 38-2 (Figs. 1, 5). This assignment agrees with the stratigraphic assignment of this layer by Keller *et al.*

(1987) and with the relative abundances of microspherule types at these sites (Fig. 3). Our analyses indicate that late Eocene occurrences of microtektites and related crystal bearing microspherules can be assigned to a given horizon on the basis of populational compositional similarity.

## DISCUSSION

Our analyses show that major element compositional overlap exists between individual microspherules of the *G. semiinvoluta* Zone and lower *Gl. cerroazulensis* Zone layers, and to a lesser extent, between those of the *G. semiinvoluta* Zone layer and of the North American layer (Figs. 2, 4, 5). However, major element compositional overlap exhibited by individual microspherules of the three late Eocene microtektite horizons does not challenge the validity of these horizons as representative of three independent microtektite events separated in time. For instance, individual microtektites of the Pleistocene Australasian strewnfield exhibit striking compositional overlap with those of the late Eocene North American strewnfield and, to a lesser extent, with those of the late Eocene *G. semiinvoluta* Zone horizon (Fig. 2). Microtektites of the Pleistocene Ivory Coast strewnfield display occasional compositional overlap with microtektites of the Australasian strewnfield and with microspherules of all three late Eocene horizons (Fig. 2). Yet the Australasian, Ivory Coast, and North American strewnfields are recognized as resulting from different microtektite events on the basis of age and geographic proximity (O'Keefe, 1976). Furthermore, the populations of microtektites from these separate strewnfields exhibit overlapping, but recognizably different compositional trends (Cassidy *et al.*, 1969; Glass, 1969; O'Keefe, 1976) (Fig. 1). In much the same manner, the three late Eocene horizons have been recognized as resulting from three separate microtektite events on the basis of biostratigraphic and chemostratigraphic relationships at multiple sites (Keller *et al.*, 1983, 1986, 1987; Glass *et al.*, 1985). The finding of three separate late Eocene microspherule layers is supported by — but not dependent on — demonstrable differences in major element compositional trends between the microspherule populations of the three different horizons.

If, as is generally accepted, microtektites result from the fusion of terrestrial rock or sediment by meteorite or comet impact, compositional variation within and between individual microtektites and related crystal-bearing spherules should be a function of variation in as many as four factors. These include (a) the initial composition of the impacted rock or sediment source, (b) the degree and type of weathering to which the source is subject prior to impact, (c) preferential oxide vaporization due to the impact, and (d) meteorite contamination. Given the interaction of these factors, a wide variety of microtektite and microspherule compositions is possible. Large compositional variation in a given microspherule population, such as the *G. semiinvoluta* Zone microspherule layer, could result from impact of a heterogeneous target and/or varying degrees of preferential oxide vaporization or meteorite contamination throughout the target area.

## CONCLUSIONS

1. The microspherule populations of three late Eocene microtektite strewnfields are distinguishable from each other on the basis of statistically determined major element compositional trends. The microtektite population of the North American strewnfield follows well defined compositional trends and is characterized by high

concentrations of $SiO_2$, $Al_2O_3$ and $TiO_2$. The microspherule population of the *Gl. cerroazulensis* Zone crystal-bearing microspherule layer is less homogeneous and is characterized by microspherules which are relatively enriched in FeO and MgO and relatively impoverished in $SiO_2$ and $TiO_2$. The microspherule population of the *Globigerapsis semiinvoluta* layer is highly heterogeneous and is characterized by microspherules which are relatively enriched in CaO and relatively impoverished in $Al_2O_3$ and $Na_2O$.

2. Compositional overlap between independent microspherule horizons is common and does not challenge the validity of stratigraphically separable microtektite layers as representative of different events separated in time. Individual microspherules from the *G. semiinvoluta* horizon often exhibit similar major element compositions similar to those of the other two late Eocene layers.

3. Once representative microspherule populations of the late Eocene layers have been compositionally analyzed, a late Eocene occurrence of microtektites, or related crystal-bearing microspherules, can be assigned to a given layer on the basis of compositional similarity.

## ACKNOWLEDGEMENTS

We would like to thank C. Kulick and W. Maze for their assistance in operating the electron microprobe. Thanks are also due to K. Hansen for discussion and help in reducing the raw data to an appropriate form for statistical manipulation, to B.P. Glass for his constructive criticism and to J.A. O'Keefe for stimulating discussion and continued encouragement.

## REFERENCES

**Barnes, V.E. and M.A. Barnes**, 1973. Tektites. Benchmark Papers in Geology, Dowden, Hutchinson and Ross.

**Cassidy, W.A., B.P. Glass, and B.C. Heezen**, 1969. Physical and Chemical properties of Australasian microtektites. *Journal of Geophysical Research* **74**, no. 4, 1008-1025.

**Chyi, M.S., D.A. Crerar, R.W. Carlson, and R.F. Stallard**, 1984. Hydrothermal Mn deposits of the Franciscan Assemblage, II. Isotope and trace element geochemistry and implications for hydrothermal convection at spreading centers. *Earth and Planetary Science Letters* **71**, 31-45.

**Donnelly, T.W. and E.C.T. Chao**, 1973. Microtektites of late Eocene age from the eastern Caribbean Sea. In *Initial Reports of the Deep Sea Drilling Project* **15**, 1031-1037.

**Ganapathy, R.**, 1982. Evidence for a major meteorite impact on the Earth 34 million years ago: Implications for Eocene extinctions. *Science* **216**, 885-886.

**Glass, B.P.**, 1969. Chemical composition of Ivory Coast microtektites. *Geochimica et Cosmochimica Acta* **33**, 1135-1147.

**Glass, B.P.**, 1982. Introduction to planetary geology. Cambridge University Press, 1145-1169.

**Glass, B.P.**, 1984. Multiple microtektite events in upper Eocene marine sediments? *Science* **224**, 309.

**Glass, B.P., R.N. Baker, D. Storzer, and G.A. Wagner**, 1973. North American microtektites from the eastern Caribbean Sea and their fission track ages. *Earth and Planetary Science Letters* **19**, 184-192.

**Glass, B.P., C.A. Burns, J.R. Crosbie, and D.L. DuBois**, 1985. Late Eocene North American Microtektites and Clinopyroxene Bearing Spherules. *Proc. of the 16th Lunar. Planet. Sci. Conf., Part I, Journal of Geophysical Research* **90**, supplement, D175-D196.

**Glass, B.P., D.L. DuBois, and R. Ganapathy**, 1982. Relationship between an iridium anomaly and the North American microtektite layer in Core RC9-58 from the Caribbean Sea. *Journal of Geophysical Research* **87**, 425-428.

**Glass, B.P., M.B. Swincki, and P.A. Zwart**, 1979. Australasian, Ivory Coast, and North American tektite strewn fields: size, mass, and correlation with geomagnetic reversals and other earth events. *Proc. of the 10th Lunar Planet. Sci. Conf.*, 2535-2545.

**Hollister, L.S., J.A. Crisp, C.G. Kulick, W. Maze, and V.B. Sisson**, 1984. Quantitative energy-dispersive analysis of rock-forming silicates. In Microbeam Analysis 1984, ed. by A.D. Remig Jr. and J.I. Goldstein (Proc. of the 19th Annual Conf. of the Microbeam Analysis Society), San Francisco Press, 143-144.

**Imbrie, J. and T. van Andel**, 1964. Vector analysis of heavy-mineral data. *Geological Society of America Bulletin* **75**, 1131-1156.

**John, C. and B.P. Glass**, 1974. Clinopyroxene-bearing glass spherules associated with North American microtektites. *Geology* **2**, 599-602.

**Keller, G.**, 1986. Stepwise mass extinctions and impact events: Late Eocene to Early Oligocene. *Marine Micropaleontology* **10**, 267-293.

**Keller, G., S.L. D'Hondt, C.J. Orth, J.S. Gilmore, P.Q. Oliver, E.M. Shoemaker, and E. Molina**, 1987. Late Eocene impact microspherules: Stratigraphy, age, and geochemistry. *Meteoritics* **22**, 25-60.

**Keller, G., S. D'Hondt, and T.L. Vallier**, 1983. Multiple microtektite horizons in upper Eocene marine sediments: No evidence for mass extinctions. *Science* **221**, 150-152.

**Keller, G., S. D'Hondt, and T.L. Vallier**, 1984. Multiple microtektite events in upper Eocene marine sediments? *Science* **224**, 309-310.

**Ngo, H.H., G.J. Wasserburg, and B.P. Glass**, 1985. Nd and Sr isotopic composition of tektite material from Barbados and their relationship to North American tektites. *Geochimica et Cosmochimica Acta* **49**, 1479-1485.

**O'Keefe, J.A.**, 1976. Tektites and their Origin. Developments in Petrology, Elsevier Sci. Pub. Co.

**Parfenova, O.V. and O.I. Yakovlev**, 1977. Some peculiarities of selective evaporation in target rocks after meteoritic impact. In Explosion and Impact Cratering, Pergamon Press, 843-859.

**Sanfilippo, A., W.R. Riedel, B.P. Glass, and F.T. Kyte**, 1985. Late Eocene microtektites and radiolarian extinctions on Barbados. *Nature* **314**, 613-615.

**Shaw, H.F. and G.J. Wasserburg**, 1982. Age and provenance of the target materials for tektites and possible impactites as inferred from Sm-Nd and Rb-Sr systematics. *Earth and Planetary Science Letters* **60**, 155-177.

Manuscript received 7/11/86